Optics Communications 405 (2017) 152–156

Contents lists available at ScienceDirect

Optics Communications

journal homepage: www.elsevier.com/locate/optcom

Over-the-air in-band full-duplex system with hybrid RF optical and baseband digital self-interference cancellation

Yunhao Zhang [a], Longsheng Li [a], Meihua Bi [a,b], Shilin Xiao [a,*]

[a] State Key Laboratory of Advanced Optical Communication System and Networks, Shanghai Jiao Tong University, 800 Dongchuan Road, 200240 Shanghai, China
[b] College of Communication Engineering, Hangzhou Dianzi University, Xiasha Gaojiaoyuan 2rd Street, 310018 Hangzhou, China

ARTICLE INFO

Keywords:
Self-interference cancellation
In-band full-duplex
OFDM

ABSTRACT

In this paper, we propose a hybrid analog optical self-interference cancellation (OSIC) and baseband digital SIC (DSIC) system for over-the-air in-band full-duplex (IBFD) wireless communication. Analog OSIC system is based on optical delay line, electro-absorption modulation lasers (EMLs) and balanced photodetector (BPD), which has the properties of high adjusting precision and broad processing bandwidth. With the help of baseband DSIC, the cancellation depth limitation of OSIC can be mitigated so as to achieve deeper total SIC depth. Experimental results show about 20-dB depth by OSIC and 10-dB more depth by DSIC over 1GHz broad baseband, so that the signal of interest (SOI) overlapped by wideband self-interference (SI) signal is better recovered compared to the IBFD system with OSIC or DSIC only. The hybrid of OSIC and DSIC takes advantages of the merits of optical devices and digital processors to achieve deep cancellation depth over broad bandwidth.

1. Introduction

In-band full-duplex (IBFD) wireless system has been attracted as an important technology to improve the spectrum efficiency of mobile communication system [1,2]. Due to its support of bidirectional simultaneous radio frequency (RF) transmission in the same frequency band compared to frequency-division duplex (FDD) and time-division duplex (TDD) mode, IBFD takes effect in kinds of wireless systems, such as relay systems, cognitive radios and radio-over-fiber (RoF) systems [3–5]. However, as shown in Fig. 1, the co-location of transmit and receive antennas causes that partial transmit signal is received by the receive antenna itself as self-interference (SI) signal, and strongly interferes with the weak in-band signal-of-interest (SOI) received. The strong SI cannot be removed by band-pass filter or notch filter due to the band overlapping of SI and SOI signals.

To deal with this problem, self-interference cancellation (SIC) systems have been widely investigated. Typical SIC is divided into several stages, including passive suppression, active analog cancellation, and digital cancellation. Passive suppression between the transmitter and receiver uses the path loss by antenna directionality and polarization [6]. Active analog SIC is to copy an additional transmit RF signal, which is also called reference signal, and transmit it from transmitter to receiver through a reliable wired channel. The reference signal is used to subtract SI on condition that amplitude and time delay of SI and reference signal are adjusted to be matched precisely. Due to high bandwidth and adjusting precision properties of optics for analog RF processing, optical SIC (OSIC) techniques have been widely researched to enlarge cancellation bandwidth and available frequency band, such as the OSIC systems based on Mach–Zehnder modulators (MZMs) [7–9], electro-absorption modulators (EAMs) [10–13] and directly modulated lasers (DMLs) [6,14]. However, among these reported works, over-the-air RF OSIC schemes demonstrate 30dB depth over less than 100 MHz OSIC bandwidth typically, at most 200 MHz [10,11]. While there is only less than 20 dB depth over larger bandwidth, which is mainly limited by the frequency response mismatch of wireless channel for SI and wired channel for the reference signal.

In this paper, in order to improve the SIC depth over large bandwidth for better recovery of wideband SOI, we propose a hybrid analog OSIC and baseband digital SIC (DSIC) system for over-the-air IBFD wireless communication, which takes advantage of the high processing bandwidth and precision of optical devices, as well as the flexible and adaptive calculating properties of DSP. The EML-based OSIC system is employed for analog cancellation, and the DSIC is introduced adapting to OSIC system to realize mismatch compensation and deepen the total SIC depth.

* Corresponding author.
E-mail address: slxiao@sjtu.edu.cn (S. Xiao).

http://dx.doi.org/10.1016/j.optcom.2017.07.076
Received 26 June 2017; Received in revised form 24 July 2017; Accepted 27 July 2017
0030-4018/

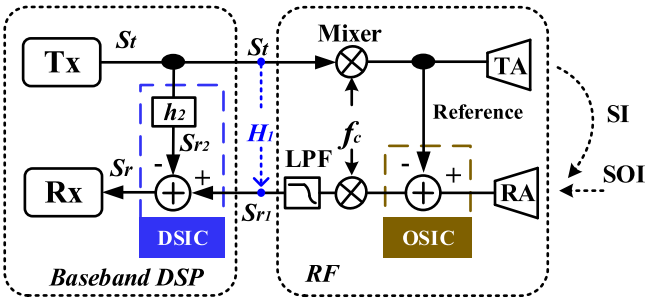

Fig. 1. Architecture of hybrid RF OSIC and baseband DSIC. Tx: transmitter; Rx: receiver; TA: transmit antenna; RA: receive antenna; LPF: low-pass filter.

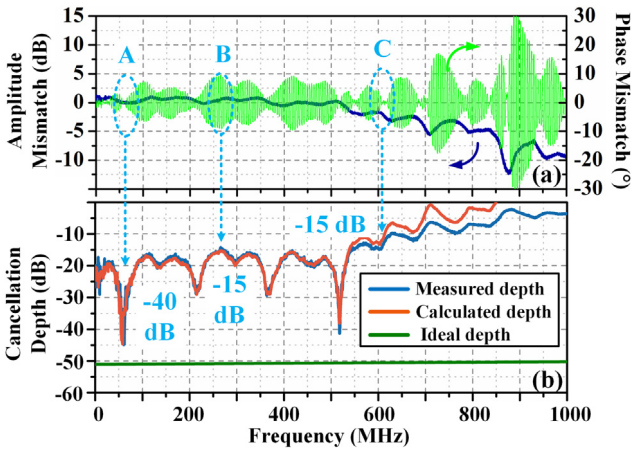

Fig. 2. (a) Frequency response mismatch of SI channel and reference channel; (b) Measured and calculated OSIC depth. (For interpretation of the references to color in this figure legend, the reader is referred to the web version of this article.)

In the following sections of this paper, we firstly analyze the limitation factors of OSIC depth and state the principle of DSIC as another cancellation. Then experimental setup and operation are discussed, following with the experimental results and analysis. Finally we conclude the paper with a summary of this work.

2. Analysis of OSIC depth limitation

In this section, we first discuss the main limitation factor of OSIC depth in order to find out the solution. Fig. 1 depicts the architecture of one IBFD user end. As our previous work, the principle of EML-based OSIC has been studied in [13]. According to the basic principle of analog SIC described in Introduction, the reference signal is transmitted through wired channel to subtract the SI signal transmitted through wireless channel, as shown in Fig. 1. For over-the-air IBFD demonstration, antennas have to be employed to transmit and receive wireless RF signals. The frequency responses of most antennas, including amplitude and phase response, are not flat with that of wired waveguides, especially in wideband scenarios. In this case, the frequency response mismatch between wired and wireless channels causes the imperfect wideband subtraction. We derive the formula of cancellation depth C towards channel response as shown in Eq. (1).

$$C = 10\lg\left[1 + (\alpha(\omega)/\beta(\omega))^2 - 2(\alpha(\omega)/\beta(\omega))\cos(\Delta\phi(\omega))\right]. \quad (1)$$

In Eq. (1), the amplitude attenuation of wired and wireless channel are represented as $\alpha(\omega)$ and $\beta(\omega)$ respectively, which are the functions of frequency ω. The phase response difference of the two channels is represented as $\Delta\varphi(\omega)$. To describe how the channel mismatch limits the analog cancellation depth over broad bandwidth, we take an example that the transmit signals have 9.85 GHz carrier and 1 GHz baseband width. The RF carrier frequency 9.85 GHz is chosen according to modulation performance of employed mixer. Moreover, 9.85 GHz is in the middle of antenna band, which represents the general situation of employed antennas. The two corresponding baseband S21 curves of wired and wireless channel are measured by Vector Network Analyzer (VNA) (KEYSIGHT N5224A), respectively. Based on these measured S21 parameters, including amplitude and phase response, the theoretical cancellation depth can be calculated according to Eq. (1). Fig. 2(a) shows the baseband amplitude and phase response mismatch, in which the phase mismatch curve is too dense to seem like a shadow region. The S21 curve after analog OSIC is also measured, then used to subtract the original S21 of SI channel to achieve the measured real analog cancellation depth, which is drawn in Fig. 2(b) as blue curve.

Moreover, the calculated theoretical OSIC depth is also shown in Fig. 2(b) as orange curve. Observed in Fig. 2(b), the theoretically calculated OSIC depth coincides well with experimentally measured OSIC depth, which proves our derivation of Eq. (1) about analog OSIC depth. According to Eq. (1), the derived cancellation depth is influenced by frequency response of two channels, so the channel mismatch is the main factor to influence analog cancellation depth. Observed in Fig. 2(a), three frequency regions are circled as Region A, B and C for example, which represent three typical cases: the low mismatch for both amplitude and phase, the low phase mismatch but high amplitude mismatch, and the low amplitude mismatch but high phase mismatch, respectively. In Region A, the OSIC depth reaches −40 dB, but only −15 dB is achieved in Region B and C. For IBFD communication, only the bands with large cancellation depth like Region A are suitable, while other bands cannot be used, but Region A only covers about 20 MHz bandwidth. This situation makes the IBFD communication with deep SIC depth limited in narrow band, which cannot fit the demand of broadband wireless communication system.

In this case, the ideal cancellation depth is derived in which there is no frequency response mismatch between wired and wireless channel, as shown in Eq. (2). Here the OSIC depth is also the function of frequency ω, and is related to the constant $\Delta\tau$ and $\Delta\alpha$, which represent the adjusting accuracy of employed optical attenuator and optical time delay line, respectively.

$$C = 10\lg\left[1 + (1+\Delta\alpha)^2 - 2(1+\Delta\alpha)\cos(\omega\Delta\tau)\right]. \quad (2)$$

The ideal cancellation curve is calculated according to Eq. (2) and shown in Fig. 2(b) as green curve. The value of $\Delta\tau$ and $\Delta\alpha$ is chosen corresponding with experimental parameters. This curve is totally near −50 dB level, which points out that the whole band can be with deep cancellation depth for IBFD if without channel mismatch. Aiming at approaching the ideal condition and faced with hard-to-change frequency response of wired and wireless channels, we focus on another subtraction in DSP after OSIC to mitigate the negative influence of channel mismatch.

3. Principle of DSIC for deeper cancellation

According to the discussion in last section, the OSIC depth and bandwidth is mainly restricted by antenna frequency response, which is hard to change. In this case, the key research point of this paper is to design a proper DSIC scheme which cooperates well with the existing OSIC systems. In order to achieve deeper total cancellation depth, DSIC scheme following OSIC conducts another subtraction of SI with the help of a finite impulse response (FIR) filter to mitigate the negative influence of mismatch.

We define the frequency and impulse response of the channel from transmitter to receiver of DSP as H_1 and h_1, respectively, as shown in Fig. 1. So the received signal Sr after DSIC is denoted as

$$Sr = Sr_1 - Sr_2 = SOI + St * h_1 - Sr_2. \quad (3)$$

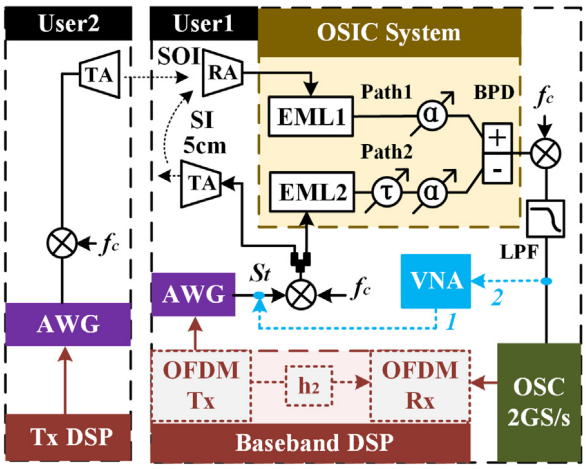

Fig. 3. Experimental setup of proposed hybrid OSIC and DSIC.

To cancel the SI and recover SOI, ideal Sr should be SOI only. So Sr_2 has to satisfy Eq. (4).

$$Sr_2 = St * h_1. \tag{4}$$

On the other hand, Sr_2 in DSIC represents the St filtered by the FIR filter h_2, so the Sr_2 is also denoted as Eq. (5).

$$Sr_2 = St * h_2. \tag{5}$$

Deduced from Eqs. (4) and (5), the h_2 should satisfy the equality to h_1, and calculated by Eq. (6).

$$h_2 = h_1 = ifft\left(H_1\right) = ifft\left(\sqrt{P_1}e^{\theta_1}\right). \tag{6}$$

The parameters P_1 and θ_1 are the power and phase response of baseband SI transmit channel, as shown in Fig. 1. They are the function of frequency which can be collected by VNA discretely. Then the DSIC calculates the filter of St with impulse response h_2, and uses it to conduct the digital subtraction for deeper total cancellation depth.

4. Experimental setup and results

4.1. Experimental setup

To verify the performance of hybrid OSIC and DSIC, experiment is conducted corresponding to the setup architecture of Fig. 3. In OSIC systems, two EMLs are employed to modulate received signal and the reference signal to optical domain, respectively. The tunable optical attenuators and time delay line are configured on the two paths, in order to align the amplitude and phase of SI and reference signals precisely before subtraction in the balanced photodetector (BPD). The detailed principle of OSIC is described in our previous work [13]. Corresponding to the case in Section 2, the carrier frequency of both SOI and SI is set to 9.85 GHz with 10 dBm power generated by microwave source. And sample rate of arbitrary waveform generator (AWG, Tektronix AWG7122C) is set 2 GS/s, namely 1 GHz baseband bandwidth of generated signal. The baseband S21 parameters are measured by VNA, including power and phase response values. The calculations of IFFT and convolution are conducted by MATLAB digitally. Both IFFT points and VNA resolution are set to 4096. Here, the 16-Quadrature Amplitude Modulation Orthogonal Frequency Division Multiplexing (16-QAM OFDM) signal is employed as transmit signal since OFDM is a popular modulation format with high bandwidth efficiency, and has been chosen as air interface waveform technology in 4G and future mobile communication system [15]. Moreover, the SIC depth of OFDM signal can be convenient to observe thanks to its flat power spectrum. For the generation of OFDM signal, the number of subcarriers and FFT points are both set 4096, corresponding to the sample point number of FIR filter impulse response $h_2(n)$. The amplitude of baseband OFDM signal is generated as 0.5 V. After mixed with carrier frequency, amplified and transmitted though wireless channel, the SI and SOI received at receive antenna are about −23 dBm and −30 dBm RF power, respectively.

4.2. Cancellation performance with hybrid OSIC and DSIC

To quantify the effectivity of hybrid OSIC and DSIC performance, we present the spectra and constellation diagrams of three conditions in Fig. 4. The spectra and constellation diagrams are drawn by MATLAB according to received signal sampled by an oscilloscope (LeCroy SDA845Zi-A) with 2 GS/s sample rate. Fig. 4(a) shows the spectrum and constellation diagram of SOI with neither OSIC nor DSIC, namely covered totally by SI. The active observed frequency band, namely the bandwidth of SI is set about 400 MHz in order to ensure the signal quality, since the OFDM signal may be distorted if its highest frequency component is closed to 1/2 sample rate. This 400 MHz bandwidth can represent the general situation in the total 1 GHz baseband. Fig. 4(b) shows the results after OSIC but without DSIC. In this case, the SI is canceled for about 15–20 dB, and the recovered SOI is with EVM of 23.2. The Sr_2 is generated according to Eq. (5), which is desired to be the same as that of residual SI signal for total subtraction. The spectrum of Sr_2 is also shown in Fig. 4(b) by dark yellow curve, which coincides well with residual SI. After subtraction in DSIC, the spectrum and constellation diagram of recovered SOI is shown in Fig. 4(c). Compared with the spectrum in Fig. 4(b), the residual SI has 10 dB more cancellation, which means the signal-to-noise ratio increases 10 dB. So the recovered SOI shows EVM of 7.6, much better than 23.2 in the case with OSIC only. This improvement of EVM proves the deeper cancellation of hybrid OSIC and DSIC than OSIC only, for about 10 dB increasing.

4.3. Cancellation performance with DSIC only

The previous results prove the inadequacy of OSIC and the solution towards it with DSIC. After 10–20 dB analog cancellation, the residual signal is sampled by analog-to-digital converter (ADC) of the oscilloscope and then subtracted in DSP devices, leading to 10 dB more cancellation depth. In order to completely show the need of hybrid OSIC and DSIC, in this subsection the necessity of OSIC is discussed. The OSIC plays the role of analog RF signal cancellation. We conduct an experiment to test whether the analog cancellation can be totally replaced by digital cancellation.

In this case, OSIC system is disabled and the channel response H_1 is measured again. According to Eqs. (3) and (4), h_2 and Sr_2 are calculated to subtract SI signal in DSP. The spectrum and constellation diagram of recovered SOI are shown in Fig. 5. Observed from Fig. 5, the DSIC achieve only less than 15 dB cancellation depth, leading to EVM value of 41.8, which is obviously a bad cancellation performance. This situation is mainly caused by the dynamic range of ADC. Before DSIC, the analog signal is converted to the digital signal through an ADC. The ADC's dynamic range at the receiver is the maximum radio between the strongest and weakest received signal power. If without analog OSIC, the dynamic range is not large enough to capture the desired SOI so that the quantization noise of the ADC can overwhelm the weak SOI [16]. So the analog OSIC is necessary to employ in order to cancel the main SI before digital sampling.

5. Conclusion

In conclusion, we have proposed a hybrid analog OSIC and baseband DSIC system for over-the-air IBFD wireless communication. For the high adjusting precision and broad bandwidth properties of optical devices, analog OSIC based on EMLs and BPD is employed. Faced with the situation that OSIC depth is mainly limited by channel response

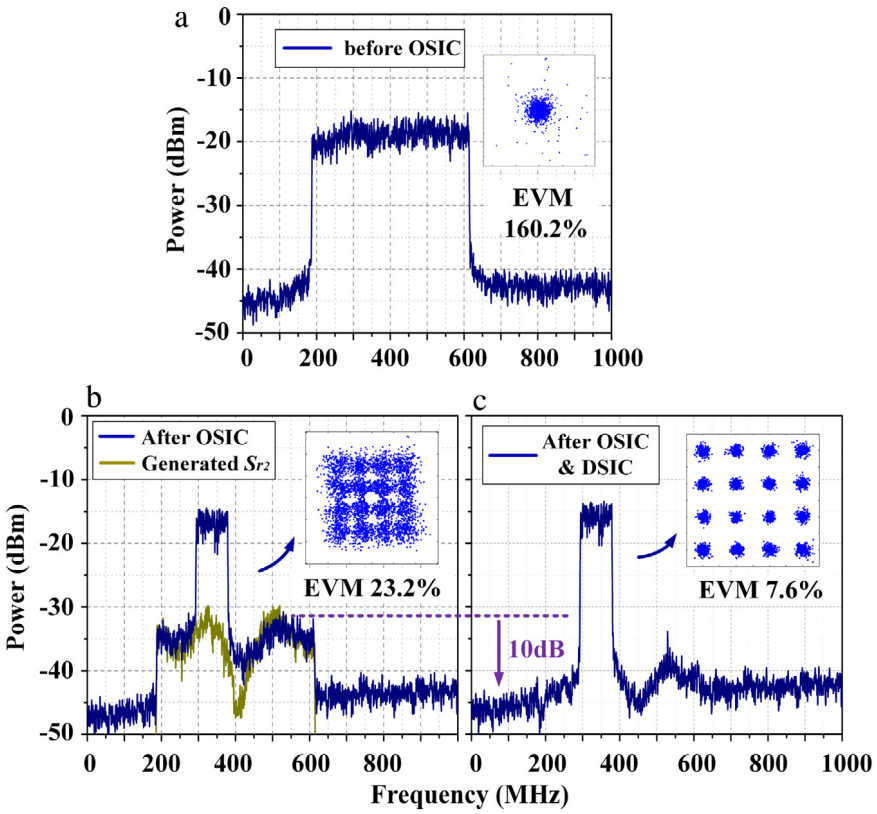

Fig. 4. Spectra and constellation diagrams of recovered SOI (a) before OSIC; (b) with OSIC but without DSIC (c) with hybrid OSIC and DSIC.

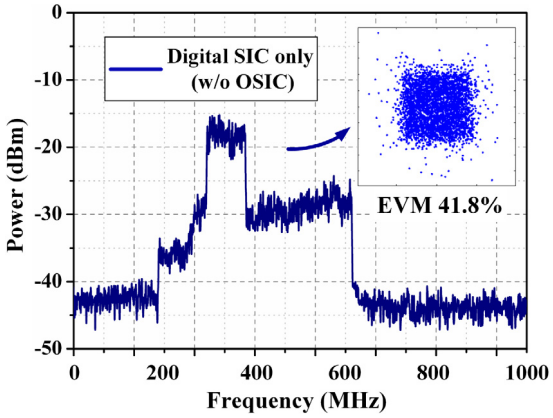

Fig. 5. Spectrum and constellation diagram of recovered SOI with DSIC only.

mismatch, baseband DSIC is designed according to OSIC condition. Experimental results show the 20 dB depth by OSIC and 10 dB more depth by DSIC, which means the SOI overlapped by SI signal is better recovered compared to the IBFD system with OSIC only. Moreover, the necessity of OSIC is experimentally studied. The results prove that the hybrid of OSIC and DSIC has the advantages of both broad cancellation bandwidth and deep cancellation depth.

Acknowledgments

This work was supported in part by the National Natural Science Foundation of China (NSFC) (61501157, 61431009), and the Natural Science Foundation of Zhejiang Province, China (Grant No. LQ16F050004).

References

[1] A. Sabharwal, P. Schniter, D. Guo, D.W. Bliss, S. Rangarajan, R. Wichman, In-band full-duplex wireless: challenges and opportunities, IEEE J. on Sel. Areas Commun. 32 (9) (2014) 1637–1652.
[2] G. Liu, F.R. Yu, H. Ji, V.C.M. Leung, Xi Li, In-band full-duplex relaying: a survey, research issues and challenges, IEEE Commun. Surveys & Tutorials 17 (2) (2015) 500–524.
[3] M. Heino, D. Korpi, T. Huusari, E.A. Rodríguez, S. Venkatasubramanian, T. Riihonen, L. Anttila, C. Icheln, K. Haneda, R. Wichman, M. Valkama, Recent advances in antenna design and interference cancellation algorithms for in-band full duplex relays, IEEE Commun. Mag. 53 (5) (2015) 91–101.
[4] M. Duarte, A. Sabharwal, V. Aggarwal, R. Jana, K.K. Ramakrishnan, C.W. Rice, N.K. Shankaranarayanan, Design and characterization of a full-duplex multi-antenna system for WiFi networks, IEEE Trans. Veh. Technol. 63 (3) (2014) 1160–1177.
[5] P. Dat, A. Kanno, N. Yamamoto, T. Kawanishi, Full-duplex transmission of LTE-A carrier aggregation signal over a bidirectional seamless fiber-millimeter-wave system, J. Lightw. Technol. 34 (2) (2016) 691–700.
[6] M.P. Chang, E.C. Blow, J.J. Sun, M.Z. Lu, P.R. Prucnal, Integrated microwave photonic circuit for self-interference cancellation, IEEE Trans. on Microwave Theory and Technol. (2017) (in press).
[7] Y. Zhang, S. Xiao, H. Feng, L. Zhang, Z. Zhou, W. Hu, Self-interference cancellation using dual-drive Mach–Zehnder modulator for in-band full-duplex radio-over-fiber system, Opt. Express 23 (26) (2015) 33205–33213.
[8] X. Han, B. Huo, Y. Shao, M. Zhao, Optical RF self-interference cancellation by using an integrated dual-parallel MZM, IEEE Photo. J. 9 (2) (2017) 1–8.
[9] W. Zhou, P. Xiang, Z. Niu, M. Wang, S. Pan, Wideband optical multipath interference cancellation based on a dispersive element, IEEE Photon. Technol. Let. 28 (8) (2016) 849–851.
[10] J.J. Sun, M.P. Chang, P.R. Prucnal, Demonstration of over-the-air RF self-interference cancellation using an optical system, IEEE Photon. Technol. Let. 29 (4) (2017) 397–400.
[11] Q. Zhou, J. Ge, M.P. Fok, Fast dynamic in-band RF self-interference cancellation for enabling efficient spectral usage, Optical Fiber Communication Conference (2017) W4B–5.
[12] M.P. Chang, M. Fok, A. Hofmaier, P.R. Prucnal, Optical analog self-interference cancellation using electro-absorption modulators, IEEE Microw. and Wireless Compon. Let. 23 (2) (2013) 99–101.

[13] Y. Zhang, S. Xiao, Y. Yu, C. Chen, M. Bi, L. Liu, W. Hu, Experimental study of wideband in-band full-duplex communication based on optical self-interference cancellation, Opt. Express 24 (26) (2016) 30139–30148.
[14] S.J. Zhang, S.L. Xiao, Y.H. Zhang, H.L. Feng, L. Zhang, Z. Zhou, Directly modulated laser based optical radio frequency self-interference cancellation system, SPIE Opt. Eng. 55 (2) (2016) 026116.
[15] Y. Xu, X. Li, J. Yu, G.K. Chang, Simple and reconfigured single-sideband OFDM RoF system, Opt. Express 24 (20) (2016) 22830–22835.
[16] N. Li, W. Zhu, H. Han, Digital interference cancellation in single channel, full duplex wireless communication, IEEE International Conference on Wireless Communications, Networking and Mobile Computing, WiCOM, (2012) pp. 1–4.